O 1s excitation and ionization processes in the CO_2 molecule studied via detection of low-energy fluorescence emission

A Kivimäki[1], J Alvarez-Ruiz[2], T J Wasowicz[3], C Callegari[4], M de Simone[1], M Alagia[1], R Richter[4] and M Coreno[5]

[1] CNR-IOM, Laboratorio TASC, 34149 Trieste, Italy
[2] Instituto de Fusión Nuclear, Universidad Politécnica de Madrid, José Gutiérrez Abascal 2, 28006 Madrid, Spain
[3] Department of Physics of Electronic Phenomena, Gdańsk University of Technology, Naturowicza 11/12, 80-233 Gdańsk, Poland
[4] Sincrotrone Trieste, Area Science Park, 34149 Trieste, Italy
[5] CNR-IMIP, Monterotondo, 00016 Roma, Italy

E-mail: kivimaki@tasc.infm.it

Abstract

Oxygen 1s excitation and ionization processes in the CO_2 molecule have been studied with dispersed and non-dispersed fluorescence spectroscopy as well as with the vacuum ultraviolet (VUV) photon–photoion coincidence technique. The intensity of the neutral O emission line at 845 nm shows particular sensitivity to core-to-Rydberg excitations and core–valence double excitations, while shape resonances are suppressed. In contrast, the partial fluorescence yield in the wavelength window 300–650 nm and the excitation functions of selected O^+ and C^+ emission lines in the wavelength range 400–500 nm display all of the absorption features. The relative intensity of ionic emission in the visible range increases towards higher photon energies, which is attributed to O 1s shake-off photoionization. VUV photon–photoion coincidence spectra reveal major contributions from the C^+ and O^+ ions and a minor contribution from C^{2+}. No conclusive changes in the intensity ratios among the different ions are observed above the O 1s threshold. The line shape of the VUV–O^+ coincidence peak in the mass spectrum carries some information on the initial core excitation.

(Some figures in this article are in colour only in the electronic version)

1. Introduction

Several kinds of electronic transitions take place at and above core-level thresholds of (simple) molecules. A core electron can be excited to an empty valence orbital or to a Rydberg orbital and/or the molecule can be ionized. Furthermore, these basic transitions can be accompanied by the simultaneous excitation or removal of a valence electron, leading to double excitations, shake-up and shake-off processes. All of the resulting core-hole states decay very fast, in the femtosecond timescale, by emitting Auger electrons or, more rarely, soft x-ray photons, or in some cases by ultrafast dissociation. In order to help the reader to follow the present study, we depict in figure 1 different core excitation and ionization processes as well as their main decay channels through electron emission. (Radiative decay and ultrafast dissociation will not be discussed in this paper.)

Information on core-hole processes has traditionally been obtained by detecting the energy taken by the molecule (photoabsorption and electron energy loss spectroscopy) or by observing any primary particle created in de-excitation events (electron, ion and soft x-ray emission spectroscopies). Ultraviolet-visible (UV-Vis) fluorescence spectroscopy does not detect any of the primary particles; hence, it does not appear particularly suitable for studies of core-electron phenomena. However, the final states of the Auger decay and soft x-ray

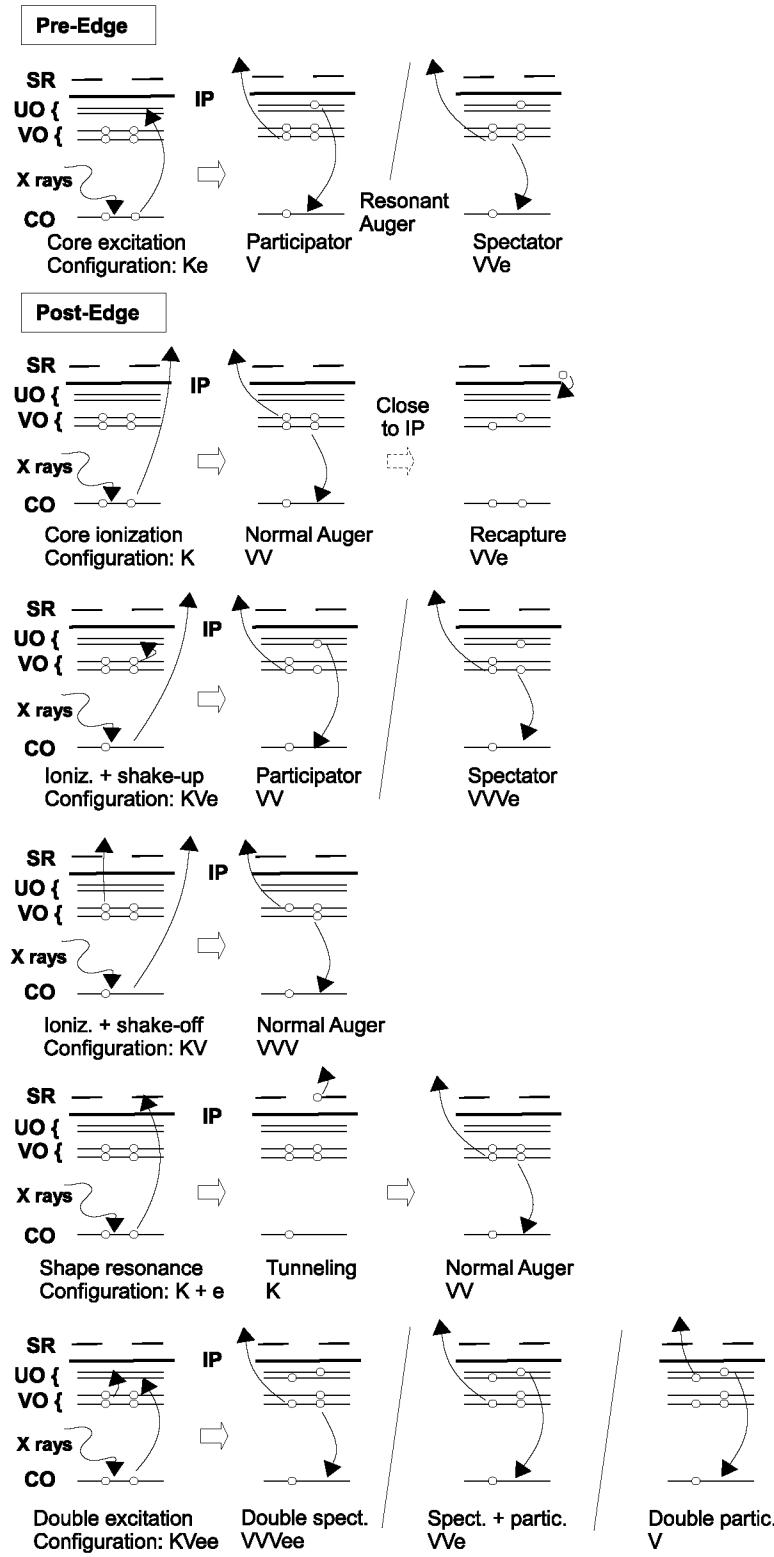

Figure 1. A simplified presentation of core excitation, core ionization and Auger decay processes. The following abbreviations are used: CO = core orbital, VO = valence orbital, UO = unoccupied orbital, IP = ionization potential, SR = shape resonance. In the designated configurations, K = core hole, V = valence hole and e = electron in an unoccupied orbital.

emission process are usually excited ones, and they may directly emit low-energy photons, or they may dissociate into excited fragments that fluoresce. Fluorescence in the VUV, UV, visible and near-infrared wavelengths generally constitutes the last step in the de-excitation pathway of core-hole states. The question is whether monitoring such emission can tell something about the process that created the initial core hole. The best chances for that occur when fluorescence

immediately follows resonant Auger decay, in which case it can be used as a high-resolution technique to study core-hole decay. For instance, this condition is fulfilled in the N_2 molecule by resonant Auger transitions from the N $1s^{-1}\pi^*$ state to the three lowest excited states of the N_2^+ ion which all can decay via fluorescence emission to the ground state of N_2^+, see e.g. [1, 2]. The situation is less promising for emission from fragments, as the same excited dissociation products can be created starting from different kinds of core-hole states. Using N_2 again as an example, the excited N^+ ion emitting at 500 nm is created at the excitations of the N 1s electron to the π^* and Rydberg orbitals, but also in the N 1s ionization continuum at the positions of the double excitations and the shape resonance [3, 4]. On the other hand, the creation of excited neutral N atoms may be limited only to the de-excitation of neutral core-hole states, including doubly excited states [4]. Therefore, the applicability of UV-Vis emission as a probe of core-electron processes greatly depends on which emission is measured as a function of photon energy.

The detection of Balmer emission, i.e. $H(n' > 2) \rightarrow H(n = 2)$ transitions in hydrogen atoms, has been particularly informative. It has been observed that Balmer emission is increased at the core-to-Rydberg excitations as compared to the core-to-valence excitations in H_2O, H_2S, NH_3 and CH_4 [5–7]. The different members of the Balmer series were found to have their intensity maxima at different photon energies: the higher the principal quantum number n' was, the closer to the core ionization potential (IP) peaked the intensity of the $H(n') \rightarrow H(n = 2)$ transition. This behaviour was explained by the spectator resonant Auger decay of the core-excited states to two-hole one-electron (2h–1e) final states (these states are designated as VVe in figure 1) whose subsequent dissociation yields excited H atoms. The excited electron may shake to another orbital of the same symmetry during resonant Auger decay, but in general 2h–1e final states with an electron on a high-n Rydberg orbital are expected when the initial core excitation promotes a core electron to a high-n Rydberg orbital. If dissociation of the molecular ion in a 2h–1e Rydberg state is adiabatic, one of the fragments gets an excited electron in a Rydberg orbital with the same principal and orbital quantum numbers [5]. In that way, highly excited H atoms can be produced by exciting molecules just below their core IPs. In the H_2O, NH_3 and CH_4 molecules also core–valence double excitations, which are located above the core IPs, appear more prominently in the excitation functions of the Lyman and Balmer emission than in the total ion yield (TIY) [8, 9]. The emission remained at an elevated level even at higher photon energies, which was attributed to fluorescence emission following the de-excitation of shake-up states to which doubly excited states converge. It was concluded that emission from excited H atoms is enhanced at any core-electron transitions that involve the population of a Rydberg orbital [8].

Coincidence experiments incorporating photon detection can bring additional information on the characteristics of fluorescence emission and on pathways leading to it. They can also help identify weak emission that cannot be resolved in conventional dispersed fluorescence measurements. Photoelectron-fluorescence (PEFCO), threshold photoelectron-fluorescence (TPEFCO) and photoion-fluorescence coincidence (PIFCO) techniques were introduced already in the 1970s [10–12]. They can be used to correlate fluorescence emission to the discrete excited state of the molecular ion and to determine the radiative lifetimes and fluorescence quantum yields of those excited states. In PEFCO spectroscopy, the electronic state of the ion is selected by the measurement of photoelectrons in the kinetic energy range of interest. TPEFCO is a variation of PEFCO where the kinetic energy is restricted to be very close to zero, only a few meV. The ionic state is instead chosen by scanning the incident photon energy. It is possible to achieve vibrational resolution with this technique. In PIFCO spectroscopy, the detection of an ion (with a time-of-flight (TOF) spectrometer) fixes the ionic species, and the specific excited state of that ion can be selected by narrowing the bandpass of the detected fluorescence. The first coincidence studies [10–12] used photomultiplier tubes (PMT) for photon detection in the UV and visible range. The application of the PIFCO technique was extended to the studies of inner-shell phenomena by Meyer *et al* [13]. They found that UV/visible photon–photoion coincidence spectra at the N 1s edge of N_2 and N_2O as well as above the I 4d edge in ICN are dominated by fragment ions, while fluorescence in the parent ion is far less important. Quite recently, Taylor and Eland [14] have combined the detection of electrons, ions and photons in a single experimental setup. By measuring ion spectra relative to electrons, but in coincidence with photons (using a PMT with 200–500 nm sensitivity range), they could improve the signal to noise ratio and observe emission in fragment and parent ions of several diatomic and triatomic molecules. The same authors have later developed an electron–electron–photon coincidence setup, where a magnetic bottle electron TOF spectrometer was used to observe an electron pair resulting from double photoionization and the above-mentioned PMT collected photons emitted by the N_2O^{2+} or CS_2^{2+} dication [15, 16]. The PIFCO technique has also been exploited to study dissociative photoionization (with) excitation, i.e. photon-induced ionization processes where the parent molecular ion dissociates and fluorescence emission occurs in an excited neutral fragment [17, 18]. In those studies, undispersed VUV photons were detected with a channeltron electron multiplier [17] or with a microchannel plate (MCP) detector [18]. Moreover, coincidences between two VUV photons, e.g. in the H_2 molecule, have been observed with an experimental setup that consists of two MCP detectors facing each other [19]. The events were attributed to neutral dissociation of doubly excited states, upon which two excited H atoms are created. Also soft x-rays have been exploited in coincidence experiments: the detection of threshold electrons in coincidence with soft x-ray emission allows one to study core photoionization at the very threshold without the post-collision interaction (PCI) effect that occurs when the core hole decays by Auger electron emission [20].

We were interested to investigate the sensitivity of fluorescence emission as a probe of core excitations in molecules that do not contain H atoms. The O 1s edge

of the CO_2 molecule is a good choice for such a study because it shows a rich collection of various core excitation phenomena. The pre-edge O 1s photoabsorption spectrum contains excitations to both valence and Rydberg orbitals, while the above-edge part reveals double excitations and shape resonances, see e.g. [21–26]. Furthermore, fragmentation of the CO_2 molecule after core excitation and core ionization has been studied extensively using different electron–ion and ion–ion coincidence spectroscopies, see e.g. [27–31], which can provide complementary information to the present investigation. We can observe the production of excited O and C atoms as well as of excited O^+ and C^+ ions, as these species have strong emission lines within the operation range (190–1000 nm) of our fluorescence spectrograph. We followed the intensity of some selected emission lines across all core excitations up to about 40 eV above the O 1s IP. Preliminary results of a neutral oxygen emission line at 845 nm were reported in [32]. We also recorded a non-dispersed fluorescence yield using a PMT. In an independent experiment, photoions were measured in coincidence with undispersed VUV photons, which gives information on the production of ions in highly excited states.

2. Experimental details

The experiments were performed at the Gas Phase Photoemission beamline [33] of the Elettra synchrotron radiation laboratory (Trieste, Italy). The beamline uses radiation from an undulator in the photon energy range of 14–900 eV. Synchrotron radiation was monochromatized by a spherical grating monochromator, equipped with a planar premirror, and sent to the experimental station. The photon energy scale was calibrated against the O 1s $\rightarrow \pi^*$ resonance of CO_2 at 535.4 eV [21].

In the dispersed and non-dispersed fluorescence experiments, a hypodermic needle was used to introduce the CO_2 gas just below the incident photon beam. The light emitted from the interaction region was collimated by a spherical Al mirror. The collimated beam exited the vacuum chamber through a quartz window and was focused with a lens onto the entrance slit of a Minuteman 305MV fluorescence spectrograph. Fluorescence light was dispersed with a 1200 lines mm^{-1} grating and detected with a liquid-nitrogen cooled CCD detector (Princeton Instruments 10:100B). The detection sensitivity curve of the experimental system was recently determined [34] and is used here. The scheme of the experimental setup was also presented in [34]. In the measurements, the incident photon energy was scanned in small energy steps in the excitation region of interest and the fluorescence spectrum was collected at each energy point typically for 5 min. The intensity of the emission line was obtained by integrating the counts over the peak. The TIY was measured simultaneously using a microsphere plate detector operating in current mode. The photodiode at the exit of the vacuum chamber monitored the photon flux for normalization purposes. An undispersed fluorescence yield of the CO_2 molecule was measured using a PMT Hamamatsu R6095 whose operation range is 300–650 nm, as given by the manufacturer. It was installed after the same exit window that was used for dispersed fluorescence experiments.

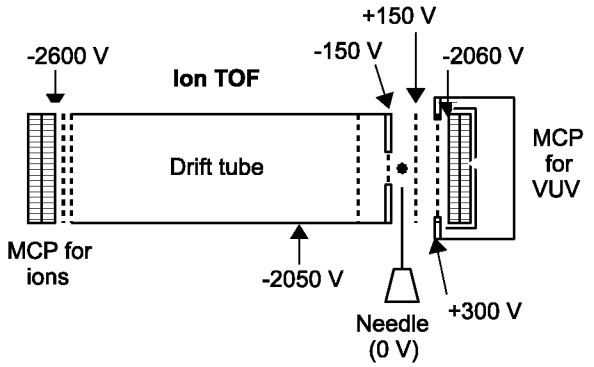

Figure 2. The scheme of the experimental setup used to measure VUV photon–photoion coincidences. The incident photon beam comes from the backside of the drawing and crosses the effusive gas jet in the interaction region, which is shown by the dot above the needle. The potentials applied to a few surfaces are given.

The ambient gas pressure in the experimental chamber was 8×10^{-5} mbar during fluorescence measurements, and it is estimated to be 10–50 times higher in the interaction region. The gas pressure was a few times higher than that in our previous experiments (e.g. [39]) because in the present study we aimed to probe processes of rather low cross sections. We cannot completely rule out the possibility that ejected photoelectrons and Auger electrons may have caused collision-induced fluorescence emission. Such contamination would affect the intensity ratios between the fragment and CO_2^+ emissions at a given photon energy as well as the intensity behaviour of a given emission line or band between the regions of a high and low photoabsorption cross section. No such effects are evident in our results, but we limit the discussion of relative intensities in the fluorescence excitation functions to a qualitative level.

During another experimental session at the Gas Phase Photoemission beamline, VUV photon–photoion coincidences were measured at the O 1s edge of the CO_2 molecule. The scheme of the experimental setup is presented in figure 2. Fluorescence photons were detected with a MCP detector. The MCP used can detect photons with wavelengths below about 150 nm. The MCP was wired for ions; hence, electrons were prevented from being detected by the high voltage at the front side of the MCP. A mesh (90% transmission) was installed in front of the MCP and set at a positive voltage (+300 V) to repel positive ions. The MCP had a diameter of 40 mm and it was located ~17 mm from the interaction region in the direction of the electric vector (**E**) of the linearly polarized incident light. Consequently, VUV photons were collected along the **E** vector within the cone whose aperture was about 100°. An ion TOF spectrometer, with a drift tube length of 105 mm, was located on the opposite side of the interaction region, also along the light polarization vector. It was operated using constant voltages that fulfilled the Wiley–McLaren space focusing condition and that allowed us to collect with 4π solid angle ions whose kinetic energies were less than ~12 eV. The signals from the detectors were fed into a time-to-digital

converter system (TMD-GPX from ACAM [35]) in order to record arrival times. The photon signal provided the start signal, while the arrival of photoions generated the stop signal. The acquisition system was configured to operate with 81 ps time resolution. Typical count rates for photoions and VUV photons were 40 000 and 200 s^{-1}, respectively. The gas pressure in the experimental chamber was about 2×10^{-6} mbar during the coincidence measurements. VUV–photoion coincidence spectra were collected usually for 45 min at each selected photon energy. Conversion of the coincidence spectra from the time scale to the mass/charge scale was achieved by the measurement of the mass spectrum of Ar with identical voltages in the ion TOF spectrometer.

3. Results and discussion

3.1. Dispersed and undispersed fluorescence experiments

The ground-state electronic configuration of the CO_2 molecule is

$$1\sigma_g^2\ 1\sigma_u^2\ 2\sigma_g^2\ 3\sigma_g^2\ 2\sigma_u^2\ 4\sigma_g^2\ 3\sigma_u^2\ 1\pi_u^4\ 1\pi_g^4\ (^1\Sigma_g^+),$$

where the $1\sigma_g$ and $1\sigma_u$ molecular orbitals (MO) correspond to the atomic O 1s orbitals. The molecule has three virtual or unoccupied valence MOs: $2\pi_u$ (often denoted as π^*), $4\sigma_u$ and $5\sigma_g$. The O 1s photoabsorption spectrum of CO_2 shows an intense resonance due to the $1\sigma_g \rightarrow 2\pi_u$ excitation at 535.4 eV [21]. The O 1s excitations to various Rydberg orbitals are also located below the O 1s edge. Their symmetries were nicely revealed by the angle-resolved ion-yield measurements of Okada *et al* [26]. Watanabe *et al* [23] applied the same technique in the O 1s continuum, showing clearly that the σ_u^* and σ_g^* shape resonances due to the $1\sigma_g \rightarrow 4\sigma_u$ and $1\sigma_u \rightarrow 5\sigma_g$ excitations appear at about 559 eV and 542 eV, respectively. These assignments have been confirmed by relaxed-core Hartree–Fock calculations of Saito *et al* [36]. A structure at ~554 eV excitation energy in the $\Sigma \rightarrow \Pi$ transition channel was also observed in [23]; it has been assigned to core–valence double excitations. Our TIY spectrum, shown as a solid line in figure 3, displays these features. Figure 3 also contains the excitation function of the 845 nm emission line, which is due to the $1s^22s^22p^33p^1(^3P) \rightarrow 1s^22s^22p^33s^1(^3S)$ transitions in neutral oxygen (a dispersed fluorescence spectrum was reported in [32]), and the partial fluorescence yield measured with the PMT that is sensitive to the light at wavelengths 300–650 nm.

Whereas the non-dispersed fluorescence yield mostly mimics the TIY curve, the excitation function of the neutral oxygen line has quite a different shape. The Rydberg excitations appear much stronger in the oxygen emission than in the TIY. It was shown in [32] that the enhancement in 845 nm emission follows resonant Auger decay of the core-excited states. The emission weakens gradually just above the O 1s IP. A similar behaviour of the same oxygen emission line at the O 1s excitations in the water molecule was previously correlated with recapture processes induced by the PCI effect [39]. The effect is general and is by no means limited to oxygen atoms. Indeed, the recent observation of metastable H atoms just above the O 1s IP of the water molecule was explained

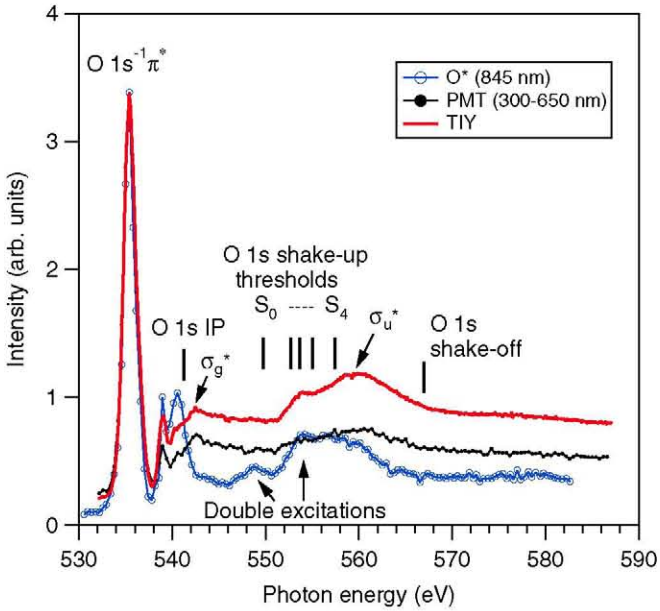

Figure 3. The excitation function of the 845 nm neutral oxygen emission line (open circles), the partial fluorescence yield in the wavelength window 300–650 nm (dots) and the total ion yield (TIY, solid line) measured across the O 1s edge of the CO_2 molecule. The curves have been scaled at the same height at the O 1s $\rightarrow \pi^*$ excitation (535.4 eV). The main spectral features are labelled. Various ionization thresholds [24, 37, 38] are also indicated. See the text for details.

using the same mechanism [40]. Briefly, just above the core IP, a fast Auger electron can overtake the slow photoelectron and push it back towards the ion where it ends up in an empty Rydberg orbital. Thus 2h–1e states can be created both below and above the O 1s threshold, and their dissociation can lead to the production of the same excited fragments. The probability of the PCI recapture decreases fast with the excess energy, which is the difference between the used photon energy and core ionization energy.

The σ_g^* shape resonance around 542 eV cannot be seen in the oxygen excitation function at all, but it is visible in the TIY and in the partial fluorescence yield. The excitation function of the oxygen emission line displays a clear feature at ~549 eV with a shoulder at ~547 eV, whereas TIY looks quite flat in the same energy range. A resonance around these energies has been observed in the yield of O^- ions [25], and it was attributed to double excitations. We concur with that interpretation. The energies of these features (547–549 eV) agree very well with those estimated for the core–valence double excited states, obtained by adding the energy of the O 1s $\rightarrow \pi^*$ excitation (535.4 eV) and the shake-up energies of 11.5–13.8 eV for the O 1s photoelectron satellites S_1–S_3, as labelled in [37] and in figure 3. In other words, the same valence-to-virtual orbital excitation is suggested to accompany both the O 1s $\rightarrow \pi^*$ transition in core–valence double excitation and O 1s photoionization in a shake-up process; the $1\pi_u \rightarrow 2\pi_u$ monopole excitation is likely involved here, similar to the case of the C 1s shake-up transitions [22]. The better-known double excitation feature around 554 eV also appears with high intensity in the excitation function of the 845 nm oxygen line.

The next feature in the excitation function of the oxygen line peaks at a lower photon energy and ends earlier than the σ_u^* shape resonance in the TIY. The differences are so clear that this feature in the excitation function of the 845 nm line may not be caused by the σ_u^* shape resonance, but more likely by other kind of electronic transitions. Maier *et al* [37] observed that the photoionization cross sections of the two unresolved O 1s shake-up satellites S_1 and S_2 experience a huge intensity increase around 6 eV kinetic energy. The shake-up energies of these satellites are about 12 eV (see figure 3). Taking into account the O 1s binding energy of 541.254 eV [24], the increased population of shake-up satellite states occurs around 559 eV photon energy, i.e. close to the maximum of the feature in the excitation function of the 845 nm oxygen line. This process would explain the differences in the resonant position and width between the excitation function of the oxygen line and TIY. If a shake-up satellite experiences a resonance, it implies that KVe types of states, where K stands for an O 1s hole, are created more abundantly (see row 3 in figure 1). Because of the electron in a virtual orbital after shake-up photoionization, subsequent Auger decay produces final states that have spectator electrons. When such final states dissociate, excited fragments may be expected. In that way, resonances in shake-up satellite cross sections may increase the number of excited fragments and, consequently, enhance fluorescence. Indeed, we suggest that the feature about 559 eV in the fluorescence yield originates at least partly from O 1s shake-up photoionization.

It appears that in CO_2 fluorescence emission from the excited oxygen atoms is less probable at the shape resonances than at double excitations. This observation can be rationalized as follows. The shape resonances decay via tunnelling to the $(O\ 1s)^{-1}$ state which further decays via normal Auger transitions (see row 5 in figure 1). The final states of normal Auger decay generally have two valence holes (and no excited electrons). On the other hand, core–valence doubly excited states can decay by resonant Auger transitions to a multitude of final states (see row 6 in figure 1). The Auger spectra of CO_2 measured at photon energies around 554 eV, corresponding to the core–valence double excitations, gave experimental evidence of transitions to VVe or VVVee final states [37]. Calculations for double excited states above the 4d ionization limit of the Xe atom predict that such decay channels are the most probable in which both the excited electrons remain as spectators [41]. Spectator electrons are thus expected to feature with high probability in the final states after Auger decay of core–valence double excitations, but much less so at the shape resonances. As discussed above, the presence of electrons in virtual orbitals (= spectator electrons) after Auger decay leads to an efficient creation of excited fragments. In the specific case of CO_2, some lowest-energy doubly charged states are quasi-stable [42], as is also indicated by the resolved vibrational structure in the recently published high-resolution Auger spectrum after C 1s ionization [43]. To the best of our knowledge, fluorescence emission has not been observed between the states of CO_2^{2+}. Thus Auger decay to quasi-stable final states probably further reduces the fluorescence emission yield at the shape resonances of CO_2. Note that the shape

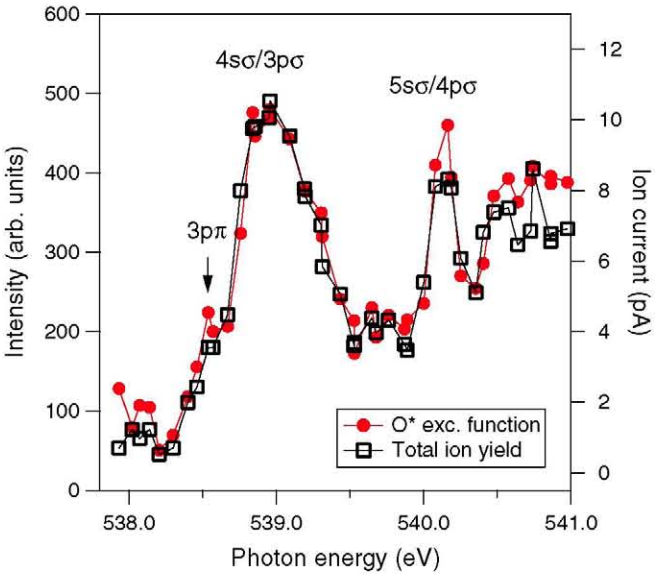

Figure 4. The excitation function of the 845 nm neutral oxygen emission line at the O 1s → Rydberg excitations in comparison with the total ion yield measured simultaneously. The assignments are according to [26].

resonances are also absent or very weak in the partial ion yields of O^- and C^- measured above the O 1s IP of CO_2 [25].

We have also remeasured with high photon energy resolution the excitation function of the 845 nm oxygen line in order to search for a possible correlation between fluorescence emission and the vibrational energy content of the core-to-Rydberg excited states. In the previous low-resolution study ($\Delta h\nu \sim 0.8$ eV) [32], the yield of this oxygen line seemed to be systematically enhanced at photon energies slightly higher than in the TIY. In the new measurements, the incident photon energy resolution was improved to about 0.15 eV and the spectral resolution for fluorescence photons was slightly relaxed to ~2.5 nm. Despite somewhat low statistics, the new results clearly show (figure 4) that the TIY and the excitation function of the oxygen line are aligned also at the Rydberg resonances around 539 eV. Thus, vibrational excitations that accompany a core-to-Rydberg electronic transition are not found to increase the probability of subsequent fluorescence emission in the oxygen atom.

The partial fluorescence yield (wavelength range 300–650 nm) from all core-to-Rydberg excitations appears reduced as compared to the TIY. This behaviour is just opposite to that of the excitation function of the 845 nm oxygen line. The most likely reason for the enhanced partial fluorescence yield at the O 1s → π^* excitation is participator decay that populates the single-hole states of the CO_2^+ ion [44, 45], followed by fluorescence emission to lower ionic states of the parent ion. In particular, the $A\,^2\Pi_u \rightarrow X\,^2\Pi_g$ emission system of CO_2^+ occurs at wavelengths between 300 and 475 nm [46] and is detected by our PMT. Participator decay from core-to-Rydberg excited states usually has a very low probability due to negligible interaction between the ionic molecular core and the electron on the diffuse Rydberg orbital. The intensity of the partial fluorescence yield at the Rydberg excitations and above the O

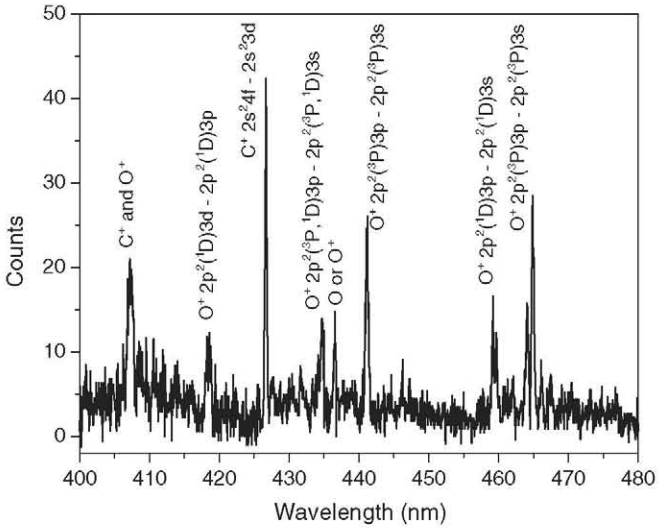

Figure 5. The fluorescence spectrum of CO_2 measured at the O 1s $\rightarrow \pi^*$ resonance after correction for relative detection efficiency. The spectrum is a composition of three measurements taken with different wavelength windows. The emission lines have been assigned using the NIST database [47].

1s edge should mostly come from excited O^+ and C^+ ions that have numerous emission lines between 300 and 650 nm [47]. Some of them could be identified in the dispersed fluorescence spectrum (figure 5) that was measured at the O 1s $\rightarrow \pi^*$ excitation.

The intensity behaviour of the emission lines in the window 422–462 nm was followed in the photon energy range 522–588 eV with 0.4 eV energy steps by measuring the emission spectrum with 2.5 nm resolution for fluorescence photons. The excitation functions obtained are shown in the upper panel of figure 6 together with TIY. All of the curves have been scaled to have the same amplitude at the O 1s $\rightarrow \pi^*$ excitation. The two O^+ peaks at 441 and 459 nm displayed similar trends; hence, only their sum is reported. All of the excitation functions show the double excitation feature at 554 eV and the shape resonance around 559 eV. The excitation function of the measured C^+ line also resonates just above the O 1s IP, which may be due to the σ_g^* shape resonance. These findings imply that the production of excited ions is possible after shape resonance excitation, its subsequent decay and dissociation. At photon energies above 570 eV, one can observe that all of the excitation functions of the ionic emitters gain strength relative to TIY. This is more clearly visible in the lower panel of figure 6, where we report the intensity ratios of the emission lines and TIY. Note that the possible photon energy dependence of the photodiode current is cancelled out in these ratios. The intensity ratios show wide maxima around 559 eV, which may be due to the σ_u^* shape resonance in the single-hole photoionization cross section or the above-mentioned resonance in the shake-up satellite cross sections, and increasing trends towards the end of the studied photon energy region. These results indicate that O 1s photoionization has not reached a stable situation by ~588 eV photon energy, but relative strengths between different photoionization channels still vary. In particular,

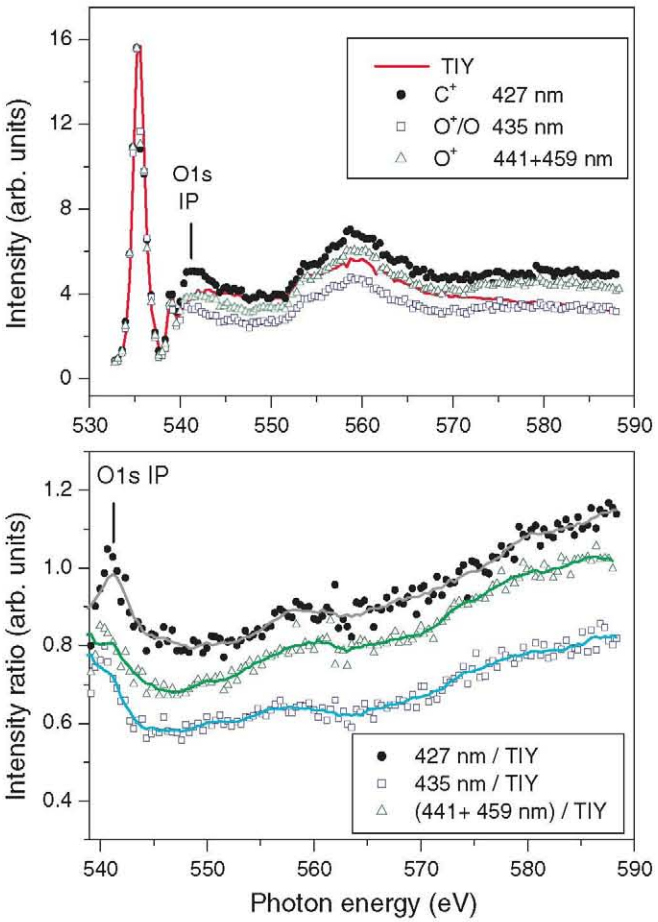

Figure 6. Upper panel: total ion yield (TIY) and the excitation functions of some emission lines observed in figure 3. Lower panel: the ratios of the excitation functions and TIY. The solid curves show the data smoothed over seven adjacent points.

shake-up and shake-off ionization channels may still evolve. Maier *et al* [37] identified several shake-up satellites with binding energies in the range 552–566 eV, i.e. their thresholds overlap the double excitation feature around 554 eV and the σ_u^* shape resonance around 559 eV (see figure 3). The lowest threshold for O 1s shake-off ionization occurs at about 567 eV [38]; this channel directly populates KV states (see row 4 in figure 1). As the cross sections of the O 1s shake-up satellites mostly decrease with the increase of the photon energy [37], we attribute to shake-off photoionization the relative enhancement of the ionic emission towards higher photon energies.

3.2. *VUV photon–photoion coincidence measurements*

We studied ionic emission of CO_2 at the O 1s edge also via VUV photon–photoion coincidence experiments. Some of the measured spectra are shown in figure 7, after counting the number of arrivals in 6 ns wide windows and conversion of the time scale to the mass/charge scale. Most observed coincidences originate from VUV emission in the C^+ and O^+ ions. The small peak at $m/z = 6$ is attributed to emission from the C^{2+} ions. There are some hints of O^{2+} emission around $m/z \approx 8$, but the spectra also have some background intensity at the same position. The source of that background structure,

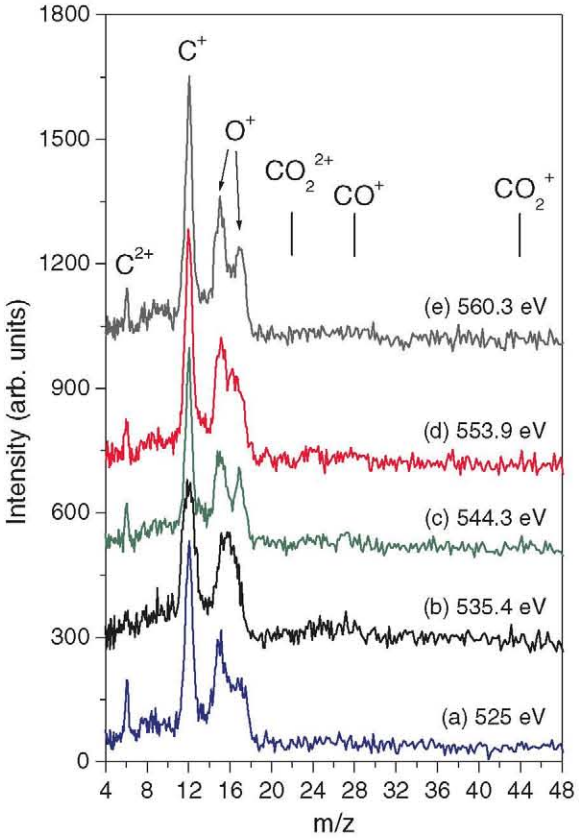

Figure 7. VUV photon–photoion coincidence spectra measured at the O 1s edge of the CO_2 molecule. Spectrum (a) was measured below the O 1s excitations (photon energy 525 eV), (b) at the O 1s $\rightarrow \pi^*$ excitation (535.4 eV), (c) slightly above the O 1s IP (544.3 eV), (d) at the core–valence double excitation resonance (553.9 eV) and (e) at the σ_u^* shape resonance (560.3 eV). The spectra have been scaled to have approximately the same heights and their base levels have been shifted for clarity. The observed ions are labelled and the expected positions of the CO_2^+, CO^+ and CO_2^{2+} ions are indicated.

and also of the one with m/z between 23 and 29, could not be identified, but it was clearly connected to photoionization of the sample molecules. The CO_2^+ ($m/z = 44$) and CO_2^{2+} ($m/z = 22$) ions are not observed in coincidence with VUV photons in the individual spectra within the statistical noise of the measurements. These ions are observed abundantly in the partial ion yields at the O 1s edge [25], but they do not emit in the VUV. A small CO_2^+ peak does appear if all our photon–photoion coincidence spectra are added together, corresponding to a total measuring time of about 11 h. That peak is attributed to soft x-ray emission from the core-ionized states, which directly populates the bound single-hole valence states of CO_2^+ [48]. The CO^+ ($m/z = 28$) ion does not emit either in the VUV, but it might be expected to appear in the VUV photon-coincidence spectra, as CO^+ could be produced together with a VUV-emitting O^+ (or O) when CO_2^{2+} (or CO_2^+) fragments. The fact that only trace amounts of CO^+ may be present in the VUV–ion coincidence spectra could indicate that VUV emission in O^+ is mostly correlated with complete fragmentation of the parent molecule.

Spectrum (a) in figure 7 was measured at the photon energy of 525 eV. The VUV photon–photoion coincidences predominantly originate from C 1s single-hole, shake-up and shake-off photoionizations. The contribution of direct valence ionization is deemed negligible, as practically no intensity was observed in the coincidence spectrum measured at the photon energy of 90 eV and the cross section of such processes is even smaller at $h\nu = 525$ eV. At that photon energy, the O^+ peak has two components which result from ions whose initial velocities are directed towards and away from the ion TOF spectrometer, indicating that these ions have received kinetic energy from the photodissociation reaction. The shape of the O^+ peak changes completely at the O 1s $\rightarrow \pi^*$ excitation (spectrum (b) in figure 7): the doublet peak structure of O^+ is replaced by a single, rather wide peak. This change can be explained by the observation that at this resonance most ions are ejected in the direction perpendicular to the electric vector of the linearly polarized light [23]. The underlying reason is that a $\Sigma \rightarrow \Pi$ excitation in a linear molecule occurs if the molecular axis is oriented perpendicularly to the electric vector, and this orientation is maintained during resonant Auger decay of the core-excited state and the subsequent dissociation, which are both much faster than molecular rotation. The resulting ions and/or neutrals are then pushed apart along the molecular axis in a linear molecule. However, this so-called axial recoil approximation breaks down in polyatomic linear molecules if a transition to a core-excited state induces bending vibrations in the molecule, which is the case for the core-to-π^* excited states of CO_2 [49, 50]. A partial preferentiality of the ionic expulsion along the perpendicular direction is nevertheless kept at the O 1s $\rightarrow \pi^*$ excitation [23], and this is also reflected in our experiment by the appearance of a single peak in the VUV–O^+ coincidence spectrum. In spectrum (b), the C^+ ion peak appears wider than that in the other spectra, which implies that excited C^+ ions receive most kinetic energy from dissociation at the O 1s $\rightarrow \pi^*$ excitation. Flight-time simulations (not shown) reproduce the experimental line shapes reasonably well when the C^+ and O^+ ions have the kinetic energies of 10 and 12 eV, respectively. The latter value is rather the lower energy limit and some fast O^+ ions probably escape detection. The simulation also indicated that the angular anisotropy parameter β for both ions is negative at the O 1s $\rightarrow \pi^*$ excitation. Our result for C^+ clearly differs from the value $\beta \approx 0.9$ found for fast C^+ ions (kinetic energy = 3–8 eV) in non-coincidence measurements [51]. The different β value is probably due to the fact that our experiment only observes a small fraction of all of the events, namely the events that are correlated with VUV emission from the ions.

Slightly above the O 1s IP (spectrum (c), $h\nu = 544.3$ eV), the O^+ peak is very clearly split into two components, which indicates the dominance of the Σ–Σ transitions, possibly caused by the influence of the σ_g^* resonance. This attribution agrees with the calculations of Saito *et al* [36], according to which the σ_g^* resonance extends to several eVs above the maximum position at ~542 eV. The peak shape of the O^+ ion can be simulated satisfactorily by an O^+ kinetic energy of about 10 eV and $\beta \approx 1$. The width of the C^+ peak implies the ion kinetic energies in the range 2–4 eV, but statistics

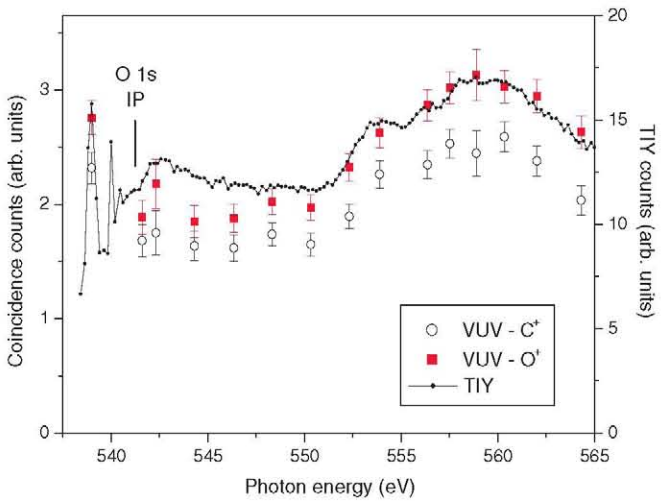

Figure 8. The intensity of VUV–C^+ and VUV–O^+ coincidences at the O 1s edge of the CO_2 molecule. Total ion yield is shown for comparison.

are too low to extract the β parameter. At the core–valence double excitation feature at ~554 eV (spectrum (d)), the two components of the O^+ peak partly merge. We ascribe this change to the excitation of core–valence doubly excited states of π symmetry [23], which enhances the ion ejection along the perpendicular direction, similar to the O 1s $\rightarrow \pi^*$ excitation. At the energies of the double excitations, however, direct O 1s photoionization is also strong, and the observed peak shape is a composition of at least these two contributions. Spectrum (e) in figure 7 was measured at the σ_u^* resonance. The O^+ peak is again split into two components, which evidences the dominance of the Σ–Σ transitions, in agreement with [36], and molecular dissociation along the **E** vector of the incident light. We thus see that the line shapes in VUV photon–photoion coincidence spectra change when different core-hole states are created by soft x-ray absorption. This also indicates that all of these core-hole processes (i.e. core excitations, shape resonances and double excitations) contribute to the VUV–O^+ signal.

Figure 8 shows the intensities of the C^+ and O^+ ions at the O 1s edge, as obtained from the fits of the VUV–photoion coincidence spectra, and the TIY measured with the ion TOF spectrometer. Both the C^+ and O^+ peaks were fitted with two Gaussian profiles in order to reproduce better the experimental data. The coincidence data points for the C^+ and O^+ ions display a similar behaviour and follow the TIY, except perhaps for the region just above the O 1s IP, where VUV emission from the ions appears slightly reduced. No conclusive effects on the ratio of excited C^+ and O^+ ions can be observed at the double excitations (around 554 eV) or at the σ_u^* resonance (around 559 eV). In fact, the C^+:O^+ intensity ratio appears to be rather constant at 0.83 ± 0.06 in all of the coincidence spectra measured above the O 1s IP. The intensity of the C^{2+} emission is too weak to draw detailed conclusions on its behaviour in the O 1s continuum. However, the branching ratio of C^{2+} emission to all ionic VUV emission was smallest at the O 1s $\rightarrow \pi^*$ excitation (spectrum (b) in figure 7) and largest at $h\nu = 525$ eV (spectrum (a) in figure 7), i.e. following C 1s ionization processes.

We briefly consider de-excitation processes that can lead to VUV emission in ionic fragments. Following single-hole core ionization (both O 1s and C 1s) in CO_2, normal Auger transitions also populate such dicationic final states that have one or two holes in the inner-valence MOs [52]. The inner-valence photoelectron spectrum of CO_2 is very complicated and cannot be described using single-electron configurations [53]. Nevertheless, in the simplest MO approximation, the inner-valence MOs of CO_2 have significant contributions from the O 2s and/or C 2s atomic orbitals. Consequently, when doubly charged states with inner-valence vacancies dissociate, one can expect that C^+ and O^+ ions with 2s holes are produced. The NIST tables [47] list numerous transitions in the VUV region for the O^+ ion with the upper-state electron configuration $2s^1 2p^4$ (for instance, $2s^1 2p^4(^4P) \rightarrow 2s^2 2p^3(^4S)$ transitions around 83 nm) and for the C^+ ion with the upper-state electron configuration of $2s^1 2p^2$ (for instance, $2s^1 2p^2(^2P) \rightarrow 2s^2 2p^1(^2P)$ transitions around 90 nm). VUV emission in the C^+ and O^+ ions is thus expected to follow normal Auger decay of the core-ionized states. Core–valence doubly excited states probably de-excite to final states having inner-valence vacancies with about the same probability as the core-ionized states do. Subsequent dissociation pathways are more complicated following core–valence double excitation, but some of them will surely result in VUV emission from the C^+ and O^+ ions having a hole in the 2s subshell. Following core–valence double excitations, VUV emission may also be expected from ionic states that have electrons on Rydberg orbitals. The O^+ ion, in particular, has several states with electron configurations such as $2s^2 2p^2 3d^1$ and $2s^2 2p^2 3s^1$ that emit in the VUV region [47]. However, the population of such ionic states may not be significant after dissociation, as the $2\pi_u$ (π^*) orbital, which is most likely involved in these core–valence doubly excited states, is built from the atomic C 2p and O 2p orbitals [54]. It appears therefore plausible that also in the case of core–valence double excitations the main decay channel resulting in VUV emission from the C^+ and O^+ ions is the one that leaves inner-valence holes in the Auger final states. This reasoning may explain the similar normalized intensities at the shape resonances and core–valence double excitations when VUV emission from the C^+ and O^+ ions is concerned.

4. Conclusions

We have studied excitation and ionization processes at the O 1s edge of the CO_2 molecule by monitoring subsequent dissociation pathways that involve the emission of low-energy photons. The emission line at ~845 nm due to a neutral oxygen atom is most enhanced at core-to-Rydberg and at core–valence double excitations, but appears much reduced or even negligible at the σ_g^* and σ_u^* shape resonances around 542 and 559 eV, respectively. The oxygen emission is suggested to gain intensity again when O 1s shake-up ionization channels open. In general, the observed neutral O emission likely follows when core-hole states decay via (resonant) Auger transitions to

final states that also have electrons on virtual orbitals. Instead, less excited neutral fragments are expected after the decay of the shape resonant states, as it mainly involves the population of two-hole final states (without electrons on virtual orbitals). Additionally, we have measured the partial fluorescence yield in the wavelength window 300–650 nm as well as the excitation functions of some C^+ and O^+ ionic states emitting in the visible region. They display all of the O 1s absorption features; hence, ionic emission in the visible range appears less sensitive to different core excitation processes than neutral emission. However, shake-off photoionization seems to produce much more excited ionic fragments than neutral fragments, which is deduced from the relative increase of ionic emission towards the end of the studied photon energy range, 588 eV.

The VUV photon–photoion coincidence spectra measured in this work reveal that C^+ and O^+ are the most important ionic emitters of VUV radiation at the O 1s edge of the CO_2 molecule. Their yields follow rather well the total ion yield. In other words, the partial VUV yields of different ions do not show different sensitivies to the core–valence double excitations or shape resonances. However, the line shapes in the coincidence spectra themselves, and particularly that of the VUV–O^+ coincidence peak, reflect to some extent the symmetry of the final state of the initial core excitation process that eventually leads to VUV emission. VUV photon–C^+/O^+ coincidences are suggested to originate mostly from such (resonant) Auger decay transitions that populate final states having inner-valence holes.

Acknowledgments

We are grateful to the staff of Sincrotrone Trieste and to Andrea Martin of the CNR-IOM electronic workshop for technical assistance during the beamtime. The research leading to these results has received funding from the European Community's Seventh Framework Programme (FP7/2007-2013) under grant agreement no 226716 and from the Italian National Research Council under projects MD.P06.016.002 (CNR-IOM) and MD.P03.026.001 (CNR-IMIP).

References

[1] Marquette A, Meyer M, Sirotti F and Fink R F 1999 *J. Phys. B: At. Mol. Opt. Phys.* **32** L325
[2] Ehresmann A *et al* 2006 *J. Phys. B: At. Mol. Opt. Phys.* **39** 283
[3] Marquette A, Gisselbrecht M, Benten W and Meyer M 2000 *Phys. Rev.* A **62** 022513
[4] Stankiewicz M, Melero Garcia E, Alvarez Ruiz J, Erman P, Hatherly P, Kivimäki A, Rachlew E and Rius i Riu J 2004 *Rev. Sci. Instrum.* **75** 2402
[5] Melero García E, Kivimäki A, Pettersson L G M, Álvarez Ruiz J, Coreno M, de Simone M, Richter R and Prince K C 2006 *Phys. Rev. Lett.* **96** 063003
[6] Vall-llosera G, Melero García E, Kivimäki A, Rachlew E, Coreno M, de Simone M, Richter R and Prince K C 2007 *Phys. Chem. Chem. Phys.* **9** 389
[7] Jakubowska K, Vall-llosera G, Kivimäki A, Coreno M, Melero García E, Stankiewicz M and Rachlew E 2007 *J. Phys. B: At. Mol. Opt. Phys.* **40** 1489
[8] Kivimäki A, de Simone M, Coreno M, Feyer V, Melero García E, Álvarez Ruiz J, Richter R and Prince K C 2007 *Phys. Rev.* A **75** 014503
[9] Coreno M, Kivimäki A, de Simone M, Melero García E, Vall-llosera G, Álvarez Ruiz J, Rachlew E and Stankiewicz M 2007 *Phys. Scr.* **76** C90
[10] Bloch M and Turner D W 1975 *Chem. Phys. Lett.* **30** 344
[11] Schlag E W, Frey R, Gotchev B, Peatman W B and Pollak H 1977 *Chem. Phys. Lett.* **51** 406
[12] Eland J H D, Devoret M and Leach S 1976 *Chem. Phys. Lett.* **43** 97
[13] Meyer M, Lacoursière J, Simon M, Morin P and Larzillière M 1994 *Chem. Phys.* **187** 143
[14] Taylor S and Eland J H D 2005 *Chem. Phys.* **315** 8
[15] Taylor S, Eland J H D and Hochlaf M 2006 *J. Chem. Phys.* **124** 204319
[16] Taylor S, Eland J H D and Hochlaf M 2006 *Chem. Phys.* **330** 16
[17] Wu C Y R, Chien T S, Kim C C and Judge D L 1988 *Chem. Phys. Lett.* **145** 418
[18] Kitajima M, Ukai M, Machida S, Kameta K, Kouchi N, Hatano Y, Hayaishi T and Ito K 1995 *J. Phys. B: At. Mol. Opt. Phys.* **28** L185
[19] Odagiri T, Murata M, Kato M and Kouchi N 2004 *J. Phys. B: At. Mol. Opt. Phys.* **37** 3909
[20] Rubensson J-E, Lüning J, Neeb M, Küpper B, Eisebitt S and Eberhardt W 1996 *Phys. Rev. Lett.* **76** 3919
[21] Wight G R and Brion C E 1974 *J. Electron Spectrosc. Relat. Phenom.* **3** 191
[22] Schmidbauer M, Kilcoyne A L D, Köppe H-M, Feldhaus J and Bradshaw A 1995 *Phys. Rev.* A **52** 2095
[23] Watanabe N, Adachi J, Soejima K, Shigemasa E, Yagishita A, Fominykh N G and Pavlychev A A 1997 *Phys. Rev. Lett.* **78** 4910
[24] Prince K C, Avaldi L, Coreno M, Camilloni R and de Simone M 1999 *J. Phys. B: At. Mol. Opt. Phys.* **32** 2551
[25] Öhrwall G, Sant'Anna M M, Stolte W C, Dominguez-Lopez I, Dang L T N, Schlachter A S and Lindle D W 2002 *J. Phys. B: At. Mol. Opt. Phys.* **35** 4543
[26] Okada K, Yoshida H, Senba Y, Kaminori K, Tamenori Y, Ohashi H, Ueda K and Ibuki T 2002 *Phys. Rev.* A **66** 032503
[27] Bozek J D, Saito N and Suzuki I H 1995 *Phys. Rev.* A **51** 4563
[28] Hatherly P A, Codling K, Stankiewicz M and Roper M 1995 *J. Phys. B: At. Mol. Opt. Phys.* **28** 3249
[29] Morin P, Simon M, Miron C, Leclercq N, Kukk E, Bozek J D and Berrah N 2000 *Phys. Rev.* A **61** 050701
[30] Hatherly P A, Fisher B O, Collins D J, Stankiewicz M and Roper M D 2001 *J. Alloys Compd.* **328** 20
[31] Muramatsu Y *et al* 2002 *Phys. Rev. Lett.* **88** 133002
[32] Kivimäki A, Coreno M, Álvarez Ruiz J, de Simone M, Dampc M and Zubek M 2009 *J. Phys.: Conf. Ser.* **190** 012051
[33] Prince K C *et al* 1998 *J. Synchrotron Radiat.* **5** 565
[34] Wasowicz T J, Kivimäki A, Dampc M, Coreno M, de Simone M and Zubek M 2011 *Phys. Rev.* A **83** 033411
[35] ACAM Messelectronic GmBH. www.acam.de
[36] Saito N *et al* 2005 *J. Phys. B: At. Mol. Opt. Phys.* **38** L277
[37] Maier K, Kivimäki A, Kempgens B, Hergenhahn U, Neeb M, Rüdel A, Piancastelli M N and Bradshaw A M 1998 *Phys. Rev.* A **58** 3654
[38] Eland J H D and Feifel R 2011 private communication
[39] Kivimäki A, Coreno M, Richter R, Álvarez Ruiz J, Melero García E, de Simone M, Feyer V, Vall-llosera G and Prince K C 2006 *J. Phys. B: At. Mol. Opt. Phys.* **39** 1101
[40] Harries J R, Gejo T, Honma K, Kuniwake M, Sullivan J P, Lebech M and Azuma Y 2011 *J. Phys. B: At. Mol. Opt. Phys.* **44** 095101
[41] Aksela H, Alitalo S, Jauhiainen J, Kivimäki A, Matila T, Kylli T, Nõmmiste E and Aksela S 1999 *Phys. Rev.* A **59** R2563

[42] Slattery A E, Field T A, Ahmad M, Hall R I, Lambourne J, Penent F, Lablanquie P and Eland H D 2005 *J. Chem. Phys.* **122** 084317
[43] Püttner R, Sekushin V, Kaindl G, Liu X-J, Fukusawa H, Ueda K, Tanaka K, Hoshino M and Tanaka H 2008 *J. Phys. B: At. Mol. Opt. Phys.* **41** 045103
[44] Carroll T X and Thomas T D 1991 *J. Chem. Phys.* **94** 11
[45] Piancastelli M N, Kivimäki A, Kempgens B, Neeb M, Maier K and Bradshaw A M 1997 *Chem. Phys. Lett.* **274** 13
[46] Lee L C and Judge D L 1972 *J. Chem. Phys.* **57** 4443
[47] Ralchenko Yu, Kramida A E, Reader J and NIST ASD Team 2010 *NIST Atomic Spectra Database (version 4.0.1)* available at http://physics.nist.gov/asd
[48] Gunnelin K, Glans P, Skytt P, Guo J-H, Nordgren J and Ågren H 1998 *Phys. Rev.* A **57** 864
[49] Adachi J, Kosugi N, Shigemasa E and Yagishita A 1996 *J. Phys. Chem.* **100** 19783
[50] Muramatsu Y, Shimizu Y, Yoshida H, Okada K, Saito B, Koyano I, Tanaka H and Ueda K 2000 *Chem. Phys. Lett.* **330** 91
[51] Saito N *et al* 2000 *Phys. Rev.* A **62** 042503
[52] Ågren H 1981 *J. Chem. Phys.* **75** 1267
[53] Freund H-J, Kossmann H and Schmidt V 1986 *Chem. Phys. Lett.* **123** 463
[54] Harris D C and Bertolucci M D 1989 *Symmetry and Spectroscopy: An Introduction to Vibrational and Electronic Spectroscopy* (New York: Dover)